Optimized PID control of depth of hypnosis in anesthesia

Fabrizio Padula[1] Clara Ionescu[2] Nicola Latronico[3,4]
Massimiliano Paltenghi[4] Antonio Visioli[5§] Giulio Vivacqua[5]

[1] Department of Mathematics and Statistics
Curtin University, Australia
e-mail: fabrizio.padula@curtin.edu.au

[2] Department of Electrical Energy, Metals, Mechanical Constructions and Systems,
Ghent University, Belgium
e-mail: ClaraMihaela.Ionescu@UGent.be

[3] Department of Medical and Surgical Specialties,
Radiological Sciences and Public Health,
University of Brescia, Italy
e-mail: nicola.latronico@unibs.it

[4] Department of Anesthesiology, Critical Care and Emergency
Spedali Civili University Hospital, Brescia, Italy
e-mail: maxpaltenghi@gmail.com

[5]Dipartimento di Ingegneria Meccanica e Industriale
University of Brescia, Italy
e-mail: {antonio.visioli@unibs.it,g.vivacqua@studenti.unibs.it}
[§] corresponding author

Abstract

Background and Objective: This paper addresses the use of proportional-integral-derivative controllers for regulating the depth of hypnosis in anesthesia by using propofol administration and the bispectral index as a controlled variable. In fact, introducing an automatic control system might provide significant benefits for the patient in reducing the risk for under- and over-dosing.
Methods: In this study, the controller parameters are obtained through genetic algorithms by solving a min-max optimization problem. A set of 12 patient models representative of a large population variance is used to test controller robustness. The worst-case performance in the

considered population is minimized considering two different scenarios: the induction case and the maintenance case.
Results: Our results indicate that including a gain scheduling strategy enables optimal performance for induction and maintenance phases, separately. Using a single tuning to address both tasks may results in a loss of performance up to 102% in the induction phase and up to 31% in the maintenance phase. Further on, it is shown that a suitably designed low-pass filter on the controller output can handle the trade-off between the performance and the noise effect in the control variable.
Conclusions: Optimally tuned PID controllers provide a fast induction time with an acceptable overshoot and a satisfactory disturbance rejection performance during maintenance. These features make them a very good tool for comparison when other control algorithms are developed.

Keywords: Depth of hypnosis control, PID control, gain scheduling, genetic algorithms.

1 Introduction

The application of feedback control to drug dosing problems has been largely investigated in the last years (see, for example, [1]) because of the inherent socio-economic benefits. In particular, closing the loop in general anesthesia proved to be highly beneficial in reducing costs for both patient and society at large. In fact, the use of an automatic control system might provide significant benefits such as a reduction of the workload of the anesthesiologist (who has in any case to be present with a supervisory role), a reduction of the amount of drug used (which implies a faster and better recovery time of the patient in the post-operative phase) and, effectively, a more robust performance with less over- and under-dosing episodes. The net result is an increased safety for the patient (for the avoidance of limit cycles, see [2, 3, 4]).

The complex process of general anesthesia consists of combinatory effects of three different components: hypnosis, analgesia and neuromuscolar blockade. Each of these functions is regulated by means of a specific drug. In this paper we focus on the problem of regulating the depth of hypnosis (DoH) by means of the hypnotic agent propofol in a total intravenous anesthesia (TIVA) framework. The bispectral index scale from 0-100 (BIS, AspectMedical Systems, Norwood, USA) is used as a controlled variable. It gives a measure of the brain activity based on a bispectral analysis of the EEG signal coming from the patient. It was one of the first feedback suitable signals available for closed loop regulation of DoH and became very popular in clinical onset. Other devices and respective signals are available [5], e.g. the auditory evoked potential (AEP) index [6], the wavelet-based index ($\mathrm{WAV_{CNS}}$) [7, 8], the M-entropy [9] and the somatosensory evoked potentials (SEP) [10].

There are three phases of anesthesia during a standard surgery procedure. During the induction phase the patient is driven from consciousness to the required DoH. This task, which can be considered as a set-point following task from a control system point of view, should be performed as fast as possible while avoiding overshoot, in order to avoid the occurrence of a possibly dangerous hypotension [11]. Once the required level of DoH is achieved, the maintenance phase starts, in which the DoH must be kept within a desired BIS interval, in the presence of external disturbances related to surgical stimulation. When the post-surgery intervention phase is completed, the emergence phase starts, where the administration of the drug is stopped and the patient recovers consciousness.

Hence, an automatic controller for DoH has to be designed in order to deal with different tasks, i.e. set-point following and load disturbance rejection. Furthermore, the large interpatient variability implies that robustness is a necessary property in the closed loop. Additional challenges are present due to noisy BIS signal and artefacts. These imply the necessity of selecting and

designing a suitable noise filter in the control algorithm.
When closed loop regulation is envisaged, a patient model is necessary (see, for example, [12, 13]). Several pharmacokinetic-pharmacodynamic (PK/PD) models characterizing the effect of propofol on the DoH are available. A linear time invariant model describes the relation between propofol infusion rate and the effect site concentration, while a nonlinear Hill function describes the relation between the effect site concentration and the BIS index.
Many different advanced control methods have been proposed to control the DoH in the considered framework. We enumerate a few: internal model control [14], model predictive control [15, 16], fractional control [17, 18], μ-synthesis [19], fuzzy control [20, 21], neural network based control [22], and positive control [23]. However, the most classical option is still proportional-integral-derivative (PID) control, which has been also applied on real patients in several operatory modes [24]. However, the methodology employed to tune the controller parameters is often missing or vaguely described [16, 25, 26, 27, 28, 29]. In many cases, the automatic controller is active only in the maintenance phase [26, 30, 31, 32, 33] while the induction phase is handled in open loop, i.e. by means of target-controlled infusion (TCI) [25, 34]. The latter is based on the PK/PD patient model and aims at achieving a predefining plasmatic or effect site drug concentration through bolus infusion profiles. A more rigorous tuning approach has been proposed in [17], where the tuning procedure from [35] is applied to a linearized model of the system (around the operating point) to achieve a satisfactory performance and rejecting external disturbances. As the same PID parameters are used in both phases, a two-degree-of-freedom controller is employed.
Nevertheless, a rigorous approach for the tuning of PID controllers for DoH regulation is still lacking. Indeed, the PID parameters should be carefully selected in order to obtain a fast transient response without a large overshoot in the induction phase, while keeping the BIS values within the predefined interval in the maintenance phase. That is, both excessively large and excessively small values of BIS should be avoided. Awakenings from too small infusion rates should be avoided, as well as overdosing, the latter yielding cognitive impairment and post-operative delirium [11, 36, 37].
To conclude, the development of an optimization-based tuning method is necessary in order to fully understand the performance provided by PID controllers in the considered framework. Additionally, it is necessary to provide a benchmark to allow fair comparisons to other advanced DoH control methodologies.
In this paper, which is an extended version of [38], we investigate the PID tuning problem by considering different aspects that have been somewhat overlooked in the literature:

- the induction and maintenance phases are considered separately and

therefore the tuning is optimized for each phase, e.g. by means of a gain scheduling technique;

- the PID parameters are determined by considering explicitly the nonlinearity of the process, avoiding stability issues originating from approximate linear models (see [39] for the effects of nonlinearities in this context);
- the presence of a strong noise in the BIS signal is addressed by properly filtering the control variable. In fact, the tuning of the filter time constant has to be considered as part of the design of the controller.

For this purpose, in order to carry out an objective analysis, we exploit genetic algorithms (which are capable to determine a global optimum of the optimization problem in a stochastic sense [40]) in order to find the optimal PID parameters that minimize the worst-case integrated absolute error performance index over a population of 12 patients [15]. While it cannot be claimed that this set of patients is exhaustive (namely, it cannot be claimed that the provided tuning of the parameters are the optimal ones in general clinical practice), it has to be stressed that it is in any case representative of a large population such that the controller guarantees the required patient safety [15, 41, 42].
Further on, the design of the controller's low-pass filter is thoroughly analyzed. In fact, due to noisy BIS signal, unacceptable variations of the control variable might occur. For this reason, in several clinical studies where closed-loop control is employed, the BIS signal is disregarded by the controller if the signal quality index is too small (see, for example, [27, 28]), but this might represent a serious lack of information for the feedback controller. Thus, the trade-off between loss of performance (i.e. the increment of the integrated absolute error) and the reduction of infusion rate variability is investigated, as well as the loss of performance that occurs if the derivative action is not employed.
Hence, it is believed that the results shown in the paper are very useful for a thorough analysis of the use of PID controllers in the control of DoH.
The paper is organized as follows. The pharmacokinetic-pharmacodynamic model is reviewed in Section 2. The PID controller design methodology is proposed in Section 3, while the gain scheduling approach is proposed in Section 4. Results are discussed in Section 5. A conclusion section summarizes the main outcome of this paper and points to further steps.

2 Pharmacokinetic-pharmacodynamic model

The patient model describes the relationship between drug infusion rate and drug effect by means of a pharmacokinetic-pharmacodynamic model. Pharmacokinetics (PK) refer to the infusion, distribution and elimination of the

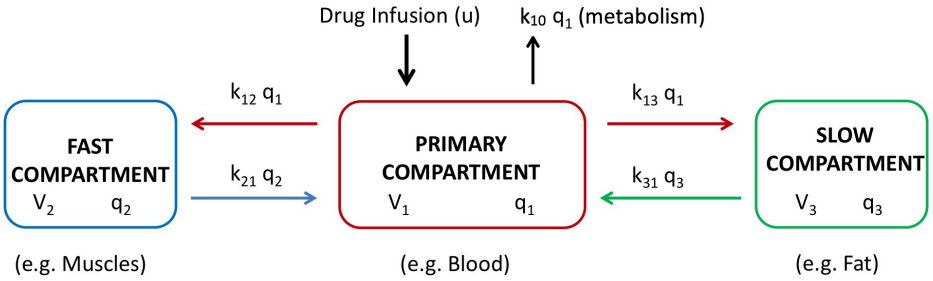

Figure 1: The mamillary three-compartmental model representing the PK of a patient.

drug in the body, while pharmacodynamics (PD) describe the relationship between effect-site concentration of a drug and its clinical effect.
The overall effect of the drug infused in the human body can be then modeled by matching the linear dynamics of the pharmacokinetics and pharmacodynamics in series with a static nonlinear function. Pharmacokinetics is usually described by means of a mamillary compartmental model, where it is assumed that each compartment presents homogeneous mixing properties, in particular the drug distribution inside a compartment is uniform. Although some simplifications have been proposed in the literature (see, for example, [13]) here the three-compartmental model typically employed for propofol is considered for the purpose of simulating patient's dynamics. A schematic block diagram is shown in Figure 1. This model is described by a first-order derivative system where mass fluxes in output for a compartment denote the input of a second or a third compartment, respectively. The general formulation of three-compartmental model is:

$$\begin{aligned} \dot{q}_1(t) &= -(k_{10} + k_{12} + k_{13})q_1(t) + k_{21}q_2(t) + k_{31}q_3(t) + u(t) \\ \dot{q}_2(t) &= k_{12}q_1(t) - k_{21}q_2(t) \\ \dot{q}_3(t) &= k_{13}q_1(t) - k_{31}q_3(t) \end{aligned} \tag{1}$$

where $q_1(t)$ [mg] expresses the quantity of the drug over the time in the central blood compartment, $q_2(t)$ [mg] denotes the quantity in the peripheral fast compartment, which includes well perfused body tissues like muscles and tendons, $q_3(t)$ [mg] expresses the amount in the slow dynamics compartment, which includes poor perfused body tissues like fat and bones, the parameters k_{ij} are constants expressing the amount of the mass flow from the ith to the jth compartment, with the exception of k_{10} which represents the elimination rate of the drug (metabolism), and $u(t)$ [mg/min] is the infusion rate of the drug into the plasmatic circulation, thus it is the input of the model.

The model parameters can be obtained as suggested in [43], where the total body weight, height and gender are used to calculate the rate transfer constants k_{ij} for $j \neq i$ [min^{-1}] by using the following equations:

$$\begin{aligned} &V_1 = 4.27, \quad V_2 = 18.9 - 0.391(age - 53), \quad V_3 = 2.38 \\ &C_{l1} = 1.89 + 0.00456(weight - 77) - 0.0681(lbm - 59) \\ &\qquad +0.02654(height - 177), \\ &C_{l2} = 1.29 - 0.024(age - 53), \quad C_{l3} = 0.0836 \\ &k_{12} = \frac{C_{l2}}{V_1}, \quad k_{13} = \frac{C_{l3}}{V_1}, \quad k_{21} = \frac{C_{l2}}{V_2}, \quad k_{31} = \frac{C_{l3}}{V_3} \end{aligned} \tag{2}$$

with V_i [L] and C_{li} [L/min] are respectively the volume and the clearance of the ith compartment and lbm is the lean body mass which can be obtained using the method of James [44] as:

$$\begin{aligned} lbm &= 1.1weight - 128\frac{weight^2}{height^2} \quad \text{for Male} \\ lbm &= 1.07weight - 148\frac{weight^2}{height^2} \quad \text{for Female} \end{aligned} \tag{3}$$

where *weight* is expressed in kilograms [kg] and *height* in centimeters [cm]. The corresponding transfer function representation can be written as:

$$PK(s) = \frac{C_p(s)}{U(s)} = \frac{1}{V_1}\frac{(s + k_{21})(s + k_{31})}{(s + p_1)(s + p_2)(s + p_3)} \tag{4}$$

where p_1, p_2, p_3 are related to k_{ij} for $i \neq j$ through:

$$\begin{cases} p_1 + p_2 + p_3 = k_{10} + k_{12} + k_{13} + k_{21} + k_{31} \\ p_1p_2 + p_1p_3 + p_2p_3 = k_{10}(k_{21}k_{31}) + k_{31}(k_{12}k_{21}) + k_{13}k_{21} \\ p_1p_2p_3 = k_{10}k_{21}k_{31} \end{cases} \tag{5}$$

The output of (4) is the plasmatic concentration of the propofol drug C_p calculated as $C_p(t) = q_1(t)/V_1$. Note that the standard error of each model parameter estimation has also been reported in [43].
Pharmacodynamics are characterized by a first-order delay-free function which relates the drug concentration in the central compartment to a fictitious volume known as *effect-site compartment*:

$$\dot{C}_e(t) = k_{1e}C_p(t) - k_{e0}C_e(t) \tag{6}$$

where C_e denotes the effect-site concentration. The presence of this compartment is motivated by a lag between the blood plasma concentration and its clinical effect. The effect-site compartment can be assumed reasonably small. In this way, the effect-site rate transfer constant will be approximately equal to the elimination rate:

$$k_{1e} \simeq k_{e0} \tag{7}$$

Hence, (6) becomes:

$$\dot{C}_e(t) = k_{e0}\left(C_p(t) - C_e(t)\right) \tag{8}$$

The corresponding transfer function is

$$PD(s) = \frac{C_e(s)}{C_p(s)} = \frac{k_{e0}}{s + k_{e0}} \tag{9}$$

Thus, the concentration in the effect compartment can be calculated from drug metabolism, described by the parameter k_{e0} [min^{-1}], which characterizes the equilibration time constant between the plasma concentration and the corresponding drug effect. Its value is estimated in the literature [43] as:

$$k_{e0} = 0.459 \tag{10}$$

Then, the relation between plasma drug concentration and clinical effect can be mathematically expressed by the means of a nonlinear sigmoid function, also known as Hill function, which models the BIS, a dimensionless parameter normalized between 0 (isoline) and 100 (fully awake and alert):

$$BIS(t) = E_0 - E_{max}\left(\frac{C_e(t)^{\gamma}}{C_e(t)^{\gamma} + C_{e_{50}}^{\gamma}}\right) \tag{11}$$

where E_0 is the baseline value representing the initial infusion-free state of the patient, $E_0 - E_{max}$ is the maximum reachable effect achieved by the infusion, γ denotes the slope of the curve (*i.e.*, the receptiveness of the patient to the drug) and $C_{e_{50}}$ is the necessary concentration of the drug to reach the half maximal effect.
Clearly, the Hill function is highly nonlinear. In fact, at the beginning of the infusion, the curve presents a *plateau*, where the presence of little quantities of the drug in the effect compartment does not affect the clinical effect until the drug concentration reaches a certain value. The final saturation expresses the impossibility to overcome the maximum achievable value E_{max} regardless of the amount of hypnotic infused.
In order to take into account the inter-patient variability, the dataset of patients presented in [15, 41, 42] has been employed. It has been defined based on clinical studies in order to represent a wide range of people and can be therefore considered as a benchmark accepted by clinicians. In addition to the set of 12 patients, a thirteenth individual has been considered as the average patient of the group, calculating for each available parameter its algebraic mean. The values of model parameters for the considered population are given in Table 1.

Id	Age	H [cm]	W [kg]	Gender	$C_{e_{50}}$	γ	E_0	E_{max}
1	40	163	54	F	6.33	2.24	98.8	94.1
2	36	163	50	F	6.76	4.29	98.6	86.0
3	28	164	52	F	8.44	4.10	91.2	80.7
4	50	163	83	F	6.44	2.18	95.9	102.0
5	28	164	60	M	4.93	2.46	94.7	85.3
6	43	163	59	F	12.00	2.42	90.2	147.0
7	37	187	75	M	8.02	2.10	92.0	104.0
8	38	174	80	F	6.56	4.12	95.5	76.4
9	41	170	70	F	6.15	6.89	89.2	63.8
10	37	167	58	F	13.70	1.65	83.1	151.0
11	42	179	78	M	4.82	1.85	91.8	77.9
12	34	172	58	F	4.95	1.84	96.2	90.8
13	38	169	65	F	7.42	3.00	93.1	96.6

Table 1: Characteristic variables for the considered set of patients (H: heigth, W: weigth).

3 Optimal tuning of PID controllers

3.1 Control scheme

We consider the standard unity feedback control scheme shown in Figure 2, where the process is the series connection of $PK(s)$, $PD(s)$ and the Hill function (see (4), (9), and (11)). The feedback controller is a PID controller in the form:

$$C(s) = K_p \left(1 + \frac{1}{sT_i} + sT_d\right) \frac{1}{(T_f s + 1)^2} \tag{12}$$

where K_p is the proportional gain, T_i is the integral time constant, T_d is the derivative time constant and T_f is the time constant of a second-order filter for the measurement noise [45]. A standard anti-windup back calculation method [32] has also been implemented although not essential for the provided tuning (see Section 3.2).

Based on the classical anesthesia regulation protocol, the initial control task is to follow the set-point step signal r from the initial BIS value E_0 of the patient to a final value BIS=50 during the induction phase. Afterwards, the control task reduces to rejecting the disturbances occuring in the maintenance phase. Although different disturbance patterns have been proposed in the literature for the controller evaluation [17, 42], the one used in [46] has been considered in this paper since it allows an easy characterization of the closed loop performance. It consists of a step signal of amplitude 10, acting directly on the process variable, followed by another step after 20

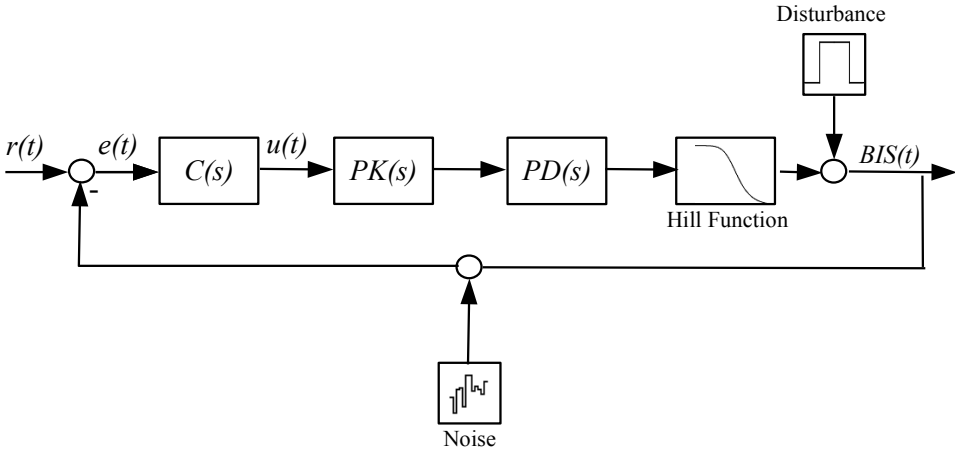

Figure 2: The considered control scheme.

minutes of amplitude -10. To mimick real BIS signal, measurement noise has been added in our simulation. In particular, an additive white Gaussian block with zero mean value and a standard deviation equal to $\sigma = 6.2721$ has been employed. The value of the standard deviation has been estimated close to that observed from real BIS data. As already mentioned, the presence of this BIS related high amplitude noise is a relevant issue and it will be analyzed in Section 3.3.

3.2 Optimal parameters

In order to determine the optimal PID controller tuning, genetic algorithms have been employed as they can guarantee (at the expense of a possibly large computational effort, which is not in any case an issue for the problem at hand) that a global optimum is obtained, at least in a stochastic sense [40]. The cost function to be minimized has been selected as the worst-case integrated absolute error for all patients (see Table 1). It is defined as

$$IAE = \int |e(t)|dt \tag{13}$$

This form is considered a suitable performance index in process control as its minimization implies in general a simultaneous reduction of both the rise time as well as the overshoot percent.
In anesthesia, the clinical outcome is considered to be satisfactory with a fast transient response without a large overshoot in the induction phase and the BIS is kept as close as possible around the desired value in the maintenance phase. Indeed, as already mentioned, both too large as well as too small values of BIS are potentially dangerous.
The optimization problem has been solved separately for the set-point following and for the disturbance rejection task, respectively. This allows the

separate investigation of the best performance achievable by the PID controller in the two phases of the anesthesia paradigm. Note that the nonlinear process has been simulated in the optimization procedure so that the Hill function has been fully taken into account for all the patients. It is also worth stressing that, with the employed procedure, the robustness of the control system is implicitly addressed because the genetic algorithm has been applied to the whole set of patients in a worst-case framework.
Further, for each control task, two different limits for the control variable have been set. Firstly, the value of 240.00 [mg/min] has been selected as an upper saturation limit, taking into account the usual clinical practice. Secondly, the value of 400.20 [mg/min] has been fixed by taking into account the maximum rate of a standard medical pump and the concentration of propofol hypnotic drug.
Initially, the noise-free case has been considered. The genetic algorithm implemented in the Matlab Global Optimization Toolbox has been employed for the optimization procedure. Results obtained are shown in Table 2 and in Figure 3 where the control variable is normalized with respect to the weight of the patient. It can be noticed that the tuning for disturbance rejection is more aggressive than for set-point following, as the proportional gain is larger and the derivative time constant is smaller. This is actually in accordance with the well-known concept for linear systems that a more aggressive controller provides a better disturbance rejection performance (namely, a larger bandwidth) at the cost of larger overshoot in the set-point step response.
Remark 1. Note that the integrator windup effect is not relevant, despite the presence of saturation. Indeed, by including an anti-windup mechanism (namely, the back-calculation structure [47]) in the optimization procedure, it turns out that the selection of the tracking time constant did not influence the final value of the cost function.
Remark 2. It is worth stressing that, because of the system nonlinearity, the optimization procedure yields a set-point dependent result. However, the selected value of the set-point (that is, a target BIS value equal to 50) is considered to be appropriate in most typical surgical procedures.

Case	Max rate [mg/min]	Worst-case IAE	Total infusion [mg]	K_p	T_i	T_d	T_f
Dist	240.0	1388	558	0.3739	1154.4009	19.3954	0.2399
Dist	400.2	1344	558	0.4446	1250.7326	20.3660	0.7204
SP	240.0	3499	281	0.0621	295.2393	29.7414	0.3041
SP	400.2	3100	279	0.0622	333.4439	34.3669	0.4986

Table 2: Optimal PID parameters for IAE minimization criteria (disturbance rejection and set-point following task). IAE and total infusion are calculated for the worst patient response among the set of patients.

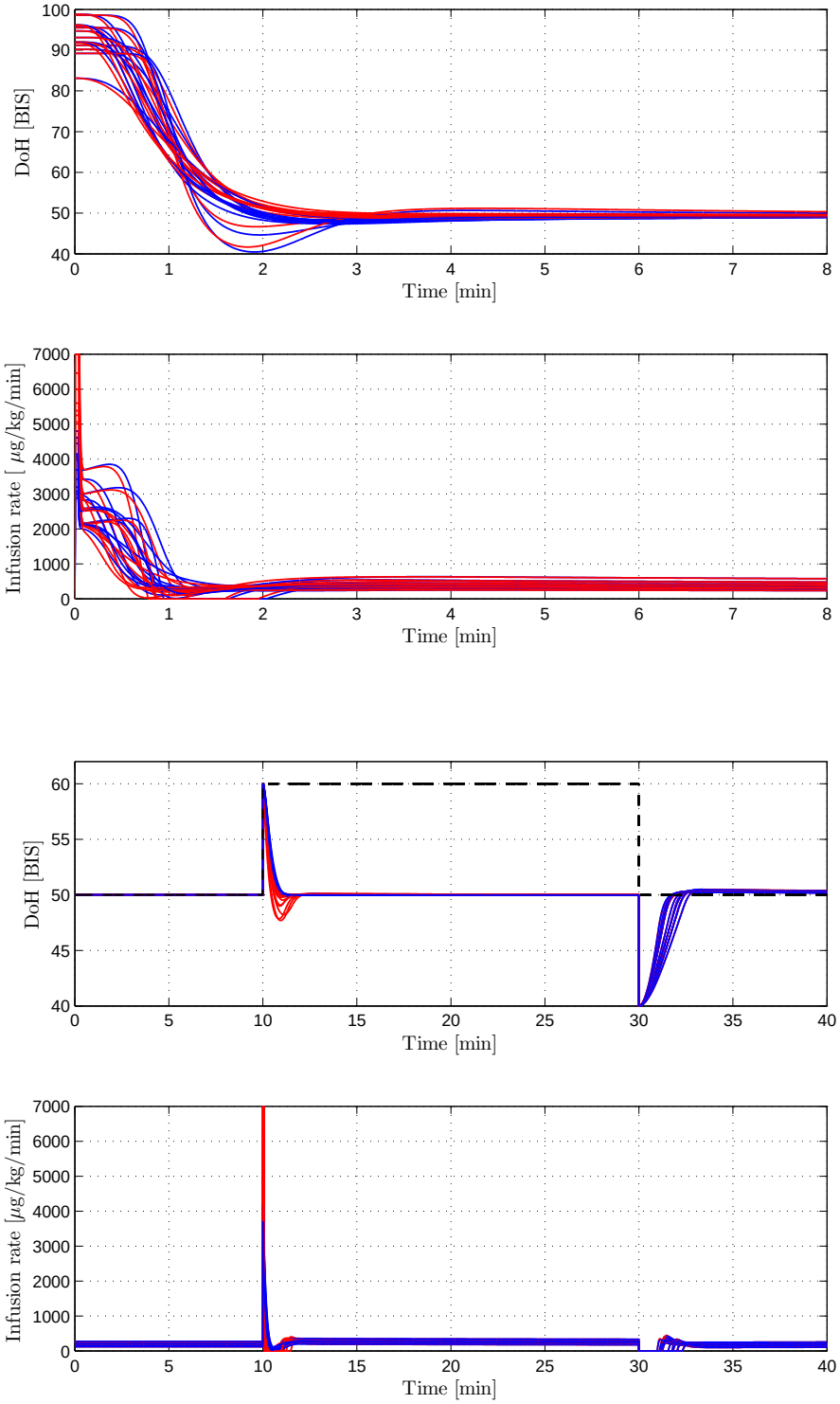

Figure 3: Simulated patients response to propofol infusion. PID controller tuned for set-point following task (top), for disturbance rejection task (bottom). Maximum infusion rate of 240.00 [mg/min] (blue), or maximum infusion rate of 400.20 [mg/min] (red).

3.3 Noise filter tuning

As already mentioned, the noise level of the BIS signal is very significant and this implies that tuning the (second-order) filter time constant T_f plays a major role in avoiding large variability in control effort, i.e. pump infusion rates. Note that the filter time constants obtained with the genetic algorithm are negligible because the system acts as a low-pass filter and therefore there are not significant changes in the IAE value if different values of T_f are considered. A simple method to tune the T_f parameter is therefore proposed in order to effectively handle the trade-off between the minimization of the IAE performance index and of the effect of noise.
The set-point following and disturbance rejection tasks are considered as two separate control problems, and the tuning obtained for the noise-free case (see Table 2) is used for the PID parameters K_p, T_i, T_d. Consequently, T_f is incremented starting from the optimal value previously obtained and, for each value, the IAE index by considering each patient of Table 1 is determined. The calculated IAE index for each value of T_f is compared with the IAE obtained by applying the optimal PID parameters in the corresponding noise-free test to the patient. Next, the worst-case between the patients is determined yielding a performance decay ratio index defined as:

$$d = \max_k \frac{IAE_{noise,k} - IAE_k}{IAE_k} \tag{14}$$

where $IAE_{noise,k}$ indicates the integrated absolute error value obtained with the selected T_f for the kth patient, and IAE_k denotes the same index calculated for the response in the noise-free case and with the optimal output-filtered PID parameters determined by the genetic algorithm. The procedure is stopped (that is, T_f is no more incremented) when an excessive overshoot in the response occurs, namely, when the BIS value falls below the threshold value of 25 in the step response. Since this may occur also for excessively small values of T_f, those values are discarded as well.
At the end of this procedure, it is possible to correlate each value of T_f and the worst-case (i.e. the biggest) performance decay obtained for the entire set of patients. It is worth stressing that different values of T_f can yield the same effect in percentage. Naturally, in those cases the greater value of T_f has to be selected as it yields the best filtering effect and ensures the same performance at the process output.
The performance decay values resulting for the different values of the filter time constant T_f are presented in Figure 4. Black circles denote the filter time constants determined for the noise-free cases, red and green stars indicate the lower and upper values of the filter parameters which result respectively in a 20% and 30% decay of the performance. Only the case with a maximum pump rate of 240.00 [mg/min] is shown for the sake of brevity, but results related to the saturation limit of 400.20 [mg/min] are

very similar.
By analyzing the obtained results, it can be observed that for low T_f values, filtering is indeed not effective. In fact, when the measurement noise enters the controller with minimum of filtering, it is amplified by the derivative action. Since we have zero mean noise, the effect of the saturation block that models the actuator has to be considered. In particular, the control variable normally operates closer to the lower saturation limit, with the result that the noise is saturated asymmetrically. In this context, process variable variations induced by the noise presence can be easily managed if they require a positive actuator reaction, but when the variation forces the BIS index to decrease, the control variable might not be able to counteract completely if the lower saturation limit is achieved. High-frequency zero mean noise thus becomes high-frequency noise with non-zero mean. In other words, the additive input is seen as a bias and the controller tries to compensate it, changing the overall closed-loop dynamics, hence perturbing the expected modeled behavior. With such a change in the control system dynamics, the determined new IAE index differs significantly from that obtained with the same parameters in the noise-free case, explaining the significant decrease of the performance. A significant change in the control system dynamics is also obviously introduced for high values of T_f and this yields an increment of the performance decay ratio.
It turns out that there are values of T_f which can ensure a satisfactory trade-off between loss of performance and effective filtering. Indeed, it is possible to realize a virtual tuning knob, that is, the tuning of the filter time constant can be performed by imposing a tolerated decay for the infusion profile. Based on clinical rationale, reasonable performance decay indices can be selected between 20% and 30%, which correspond to a balanced trade-off between the noise filtering and the optimal regulation. Furthermore, the concavity of the resulting curve offers the possibility to reach the same result with two different values of T_f. Obviously, the greatest between the two should be chosen in order to achieve a strongest noise reduction effect with the same loss of performance.
The resulting responses of the patients in the presence of noise are shown in Figure 5. The blue lines represent the results of the noise-free simulations. The red and green lines denote the results in presence of the measurement noise where the filtering time constant T_f has been chosen to assure a maximum decay performance ratio respectively of 20% and 30%.
It can be noticed that the noise effect is highly reduced even if the control variable resulting from the simulations still presents significantly high-frequency variations. As the main responsible of the noise amplification is the derivative action, it is therefore interesting to evaluate also the performance that can be obtained by considering only a PI controller.

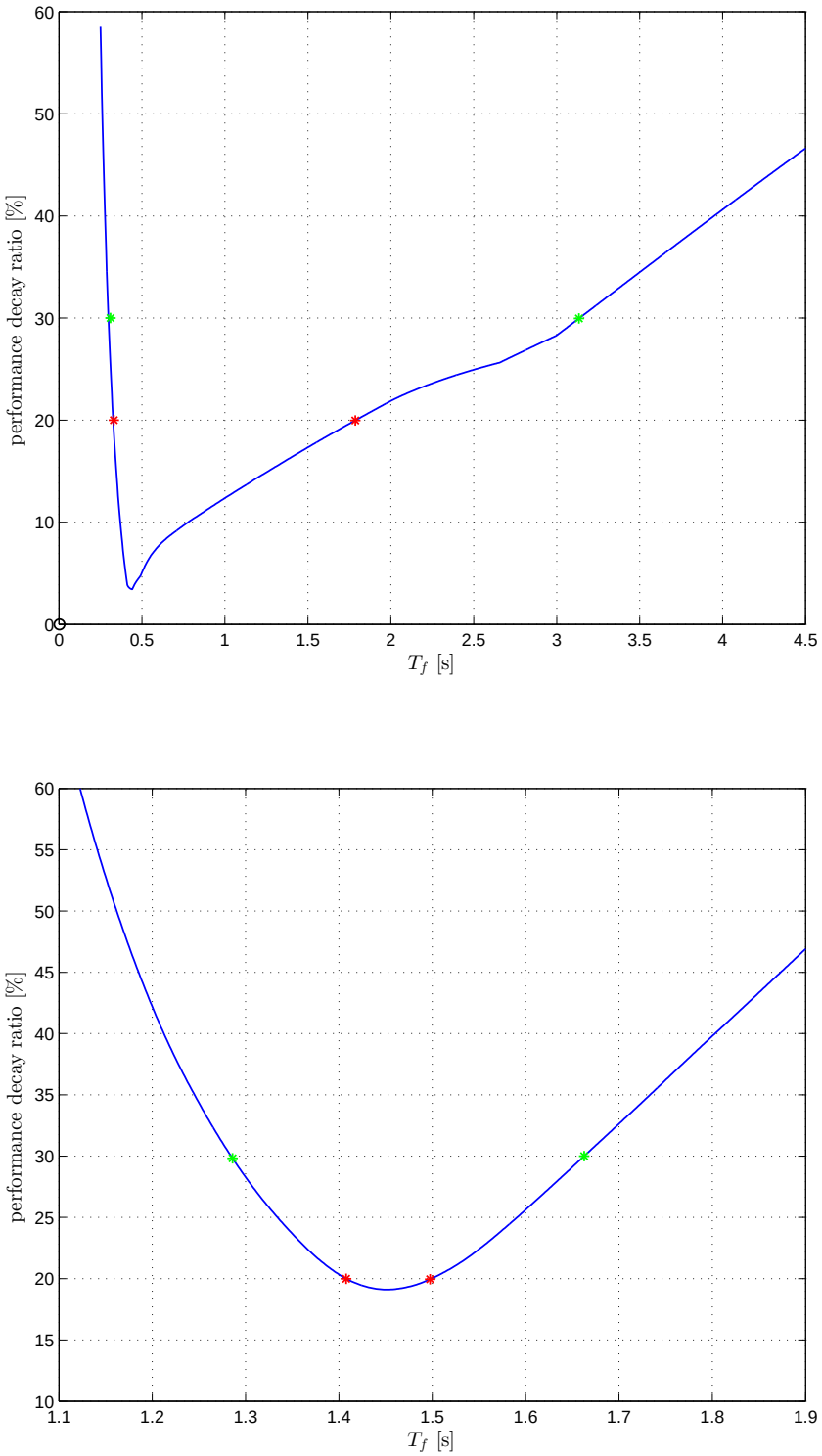

Figure 4: Simulated performance decay ratio over the filtering time constant T_f for set-point following (top) and disturbance rejection (bottom) with PID control. Maximum pump rate of 240.00 [mg/min]. Red stars: T_f parameters which lead to a decrease of 20% of IAE. Green stars: decrease of 30%. Black circle: noise-free optimal T_f parameter.

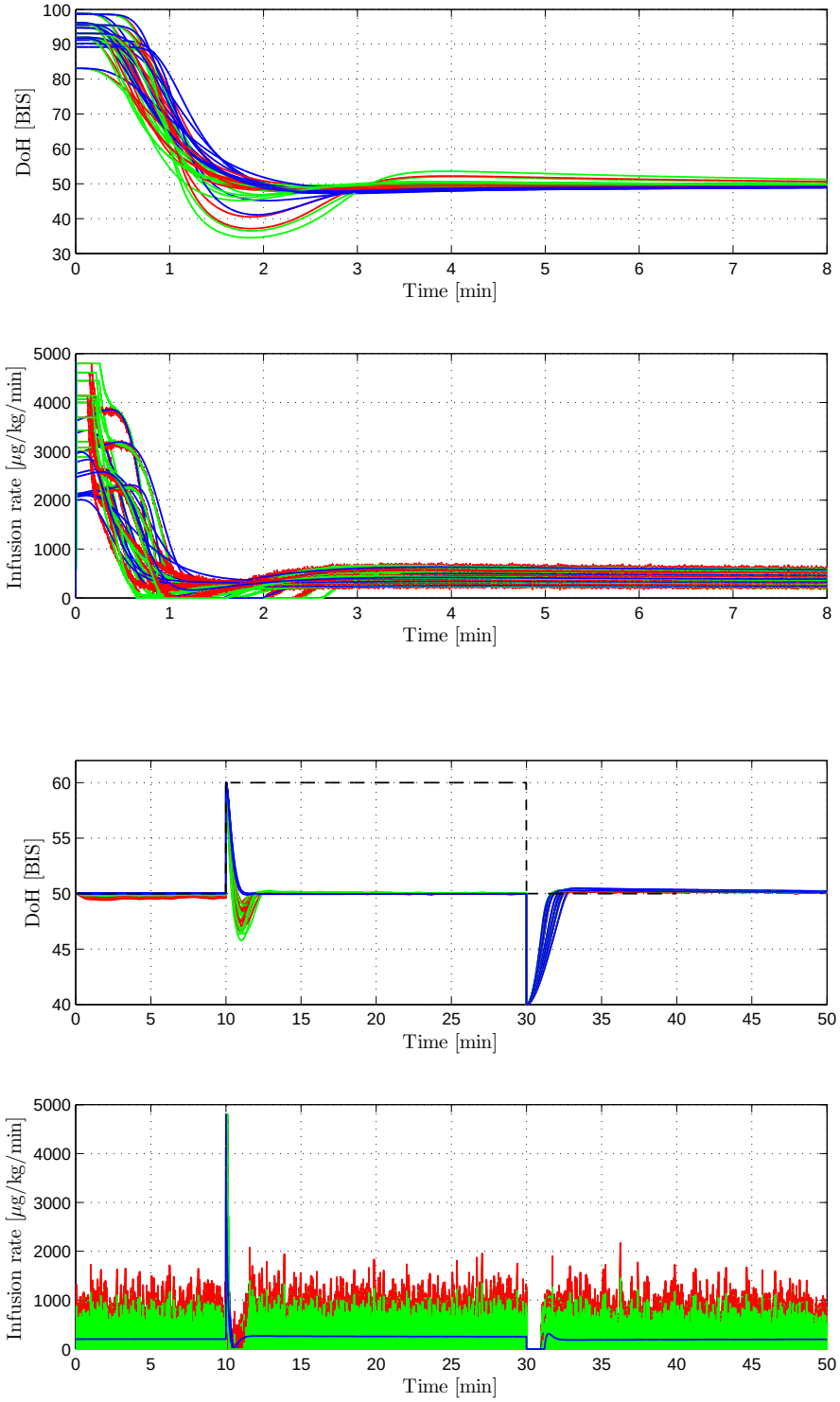

Figure 5: Simulated patients response for set-point following (top) and disturbance rejection (bottom) with PID control. Maximum pump rate of 240.00 [mg/min]. Responses in absence of noise (blue), and in presence of noise with a filtering action which leads to a maximum decay performance ratio of 20% (red) and 30% (green).

Case	Max rate [mg/min]	Worst-case IAE	Total infusion [mg]	K_p	T_i	T_f
Dist	240.0	1825	557	0.1149	1035.1358	0.0050
Dist	400.2	1819	557	0.1105	931.8496	0.0137
SP	240.0	6503	890	0.0334	314.0314	0.0062
SP	400.2	7052	885	0.0315	400.0012	0.0117

Table 3: Optimal PI parameters for IAE minimization criteria (disturbance rejection and set-point following task). IAE and total infusion are calculated for the worst patient response among the set of patients.

3.4 Optimal PI tuning

In standard process control practice it is usual to employ just a PI controller when the controlled variable is very noisy. This is also a sensible choice if the optimal PID values from Table 2 are analysed, i.e. by considering that $T_d \ll T_i$. For this reason, the same procedure employed for PID controllers has been then applied to PI controllers (i.e. setting $T_d = 0$ in (12)). The optimal tuning parameters for the noise-free case are given in Table 3 and in Figure 6. A significant difference can be observed in the (optimal worst-case) tuning related to the set-point following and the disturbance rejection tasks.
Regarding the tuning of T_f when the noise is considered (note that its value is close to zero in the noise-free case), the performance decay trends are depicted in Figure 7.
It can be noticed that the decay trend is almost linear for the set-point tracking case. In fact, as there is no derivative action and the proportional gain is small, the measurement noise is not amplified significantly even if the filter time constant assumes low values. Consequently, a bias in the process is no longer introduced. However, this occurs in the tuning for the disturbance rejection task, when the interval of the admissible values for T_f is reduced because of the constraint imposed on the maximum overshoot.
The filtering effect can be observed in Figure 8, where the patient's responses are compared in case of presence or of absence of noise, both for set-point following and disturbance rejection tasks. For the set-point following case, it turns out that the responses in the absence of noise do not significantly differ from the responses in presence of noise obtained by using the filtered controller. As expected, the tuning which causes a decrease in the performance of 30% causes a longer saturation period compared to its counterpart. On the contrary, the control variables obtained for the disturbance rejection are more affected by the noise, due to the larger proportional gain.

4 Gain scheduling

By analyzing the results of the optimal tuning methodology it can be observed that the parameters obtained for the set-point following and distur-

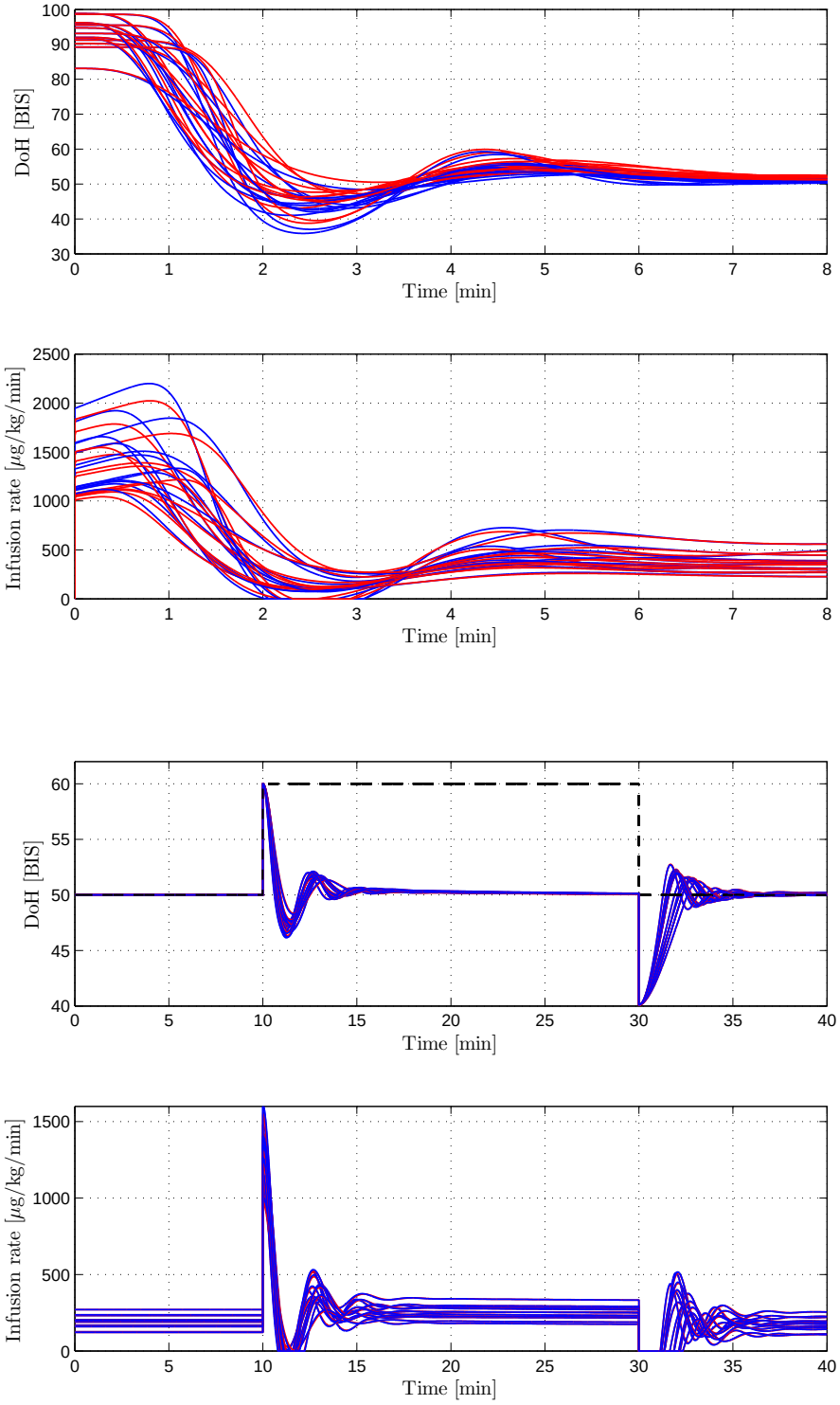

Figure 6: Simulated patients response to propofol infusion. PI controller tuned for set-point following task (top), for disturbance rejection task (bottom). Maximum infusion rate of 240.00 [mg/min] (blue), or maximum infusion rate of 400.20 [mg/min] (red).

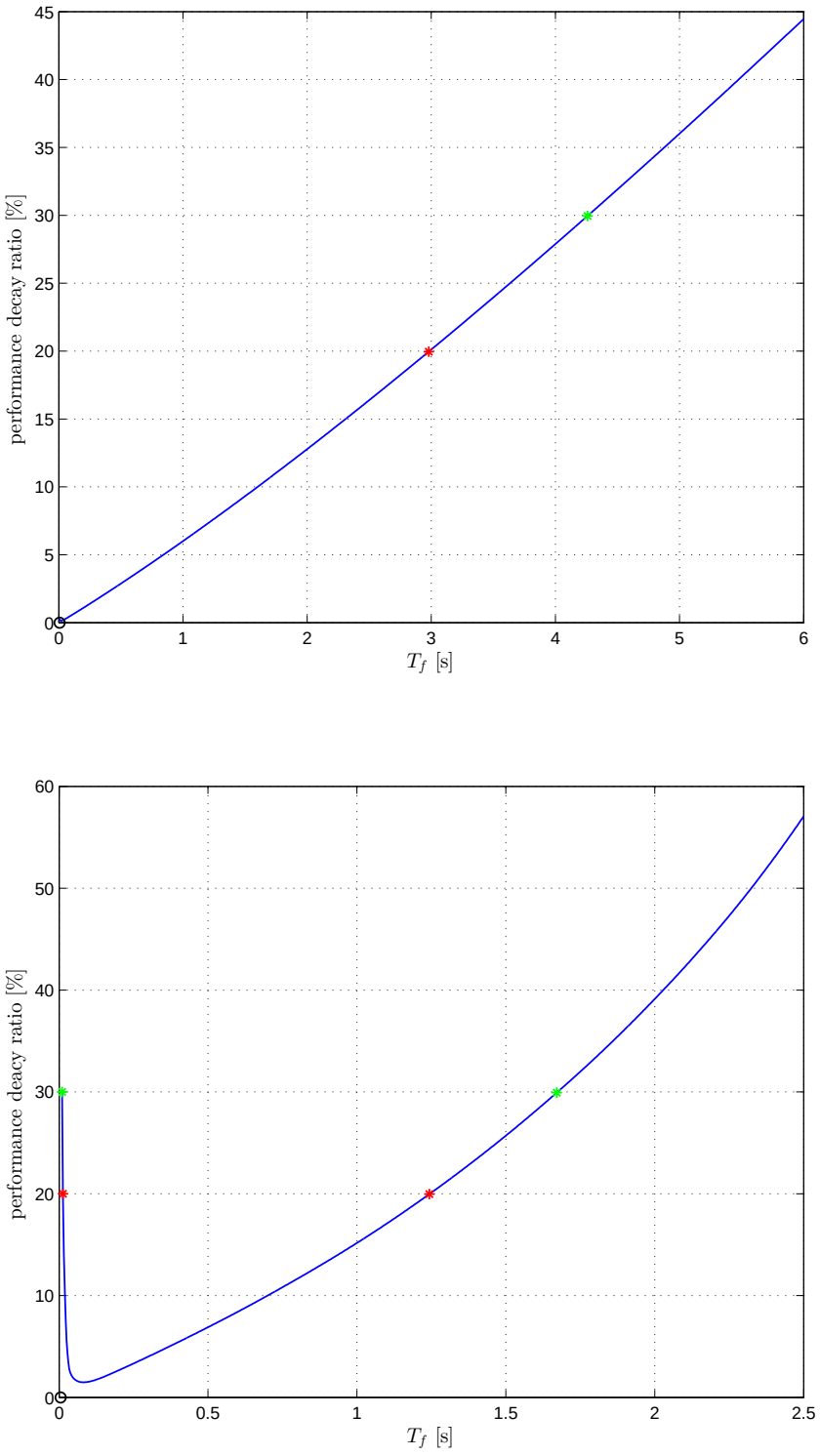

Figure 7: Simulated performance decay ratio over the filtering time constant T_f for set-point following (top) and disturbance rejection (bottom) with PI control. Maximum pump rate of 240.00 [mg/min]. Red stars: T_f parameters which lead to a decrease of 20% of IAE. Green stars: decrease of 30%. Black circle: noise-free optimal T_f parameter.

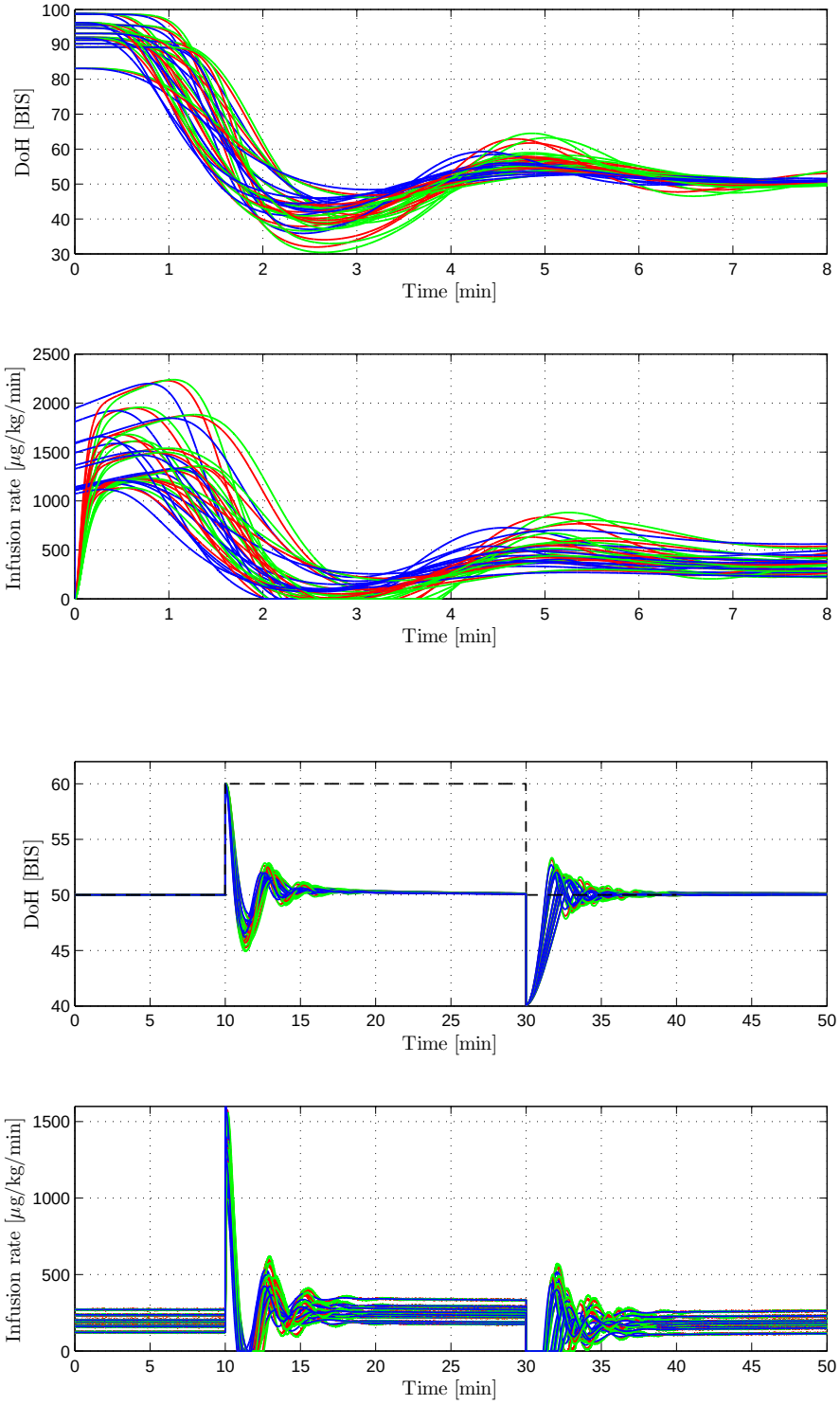

Figure 8: Simulated patients response for set-point following (top) and disturbance rejection (bottom) with PI control. Maximum pump rate of 240.00 [mg/min]. Responses in absence of noise (blue), and in presence of noise with a filtering action which leads to a maximum decay performance ratio of 20% (red) and 30% (green).

Task	Max rate [mg/min]	Worst-case IAE for Dist	Worst-case IAE for SP	Decay [%]
Dist	240.0	1825	2025	11
Dist	400.2	1819	2389	31
SP	240.0	12941	6503	99
SP	400.2	14261	7052	102

Table 4: Integral absolute error decay calculated inverting the optimal parameters for a specific task.

bance rejection tasks are significantly different. This result indicates that the use of a gain scheduling technique may be beneficial. In particular, the PI(D) controller tuned for the set-point following task is employed only during the induction phase of anesthesia. Then, when the target is attained and the DoH is stabilized around the set-point for a predefined time interval, the controller parameters are switched to the disturbance rejection optimal ones. Obviously, a bumpless switching mechanism between the two controllers has to be implemented.
In order to highlight the need of the gain scheduling strategy, the responses of the patients when the tuning for the set-point tracking task is used for disturbance rejection and vice versa are shown in Figure 9 (a PI controller for the 240.00 [mg/min] case is considered as example). It is evident that, in the induction phase, the tuning devised for the load disturbance causes in some cases a long time interval where the control variable saturates, yielding an oscillatory behaviour. The necessity of the gain scheduling technique is confirmed by analyzing Table 4 where it is shown the decay of performance obtained for the worst case between the patients in the considered set, when the PID parameters are used for the task different from that for which they have been optimized. In particular, the use of disturbance rejection tuning for set-point tracking task generates a considerable loss of performance. Indeed, because of the aggressive controller tuning, it is likely to obtain a large overshoot.

5 Discussion

The results reported in this work can be compared with those obtained by using other methodologies. In particular, the same set of patients has been investigated in [15] and in [41] where model predictive control approaches have been used. The results obtained here for induction phase suggest that the presence of derivative action is necessary for PID controller to outperform the MPC controller (as the induction phase provided by PID is faster than that provided by MPC with a very similar maximum overshoot). This is supported by the evidence of performance degradation with PI control when compared to MPC control. In the induction phase our PID con-

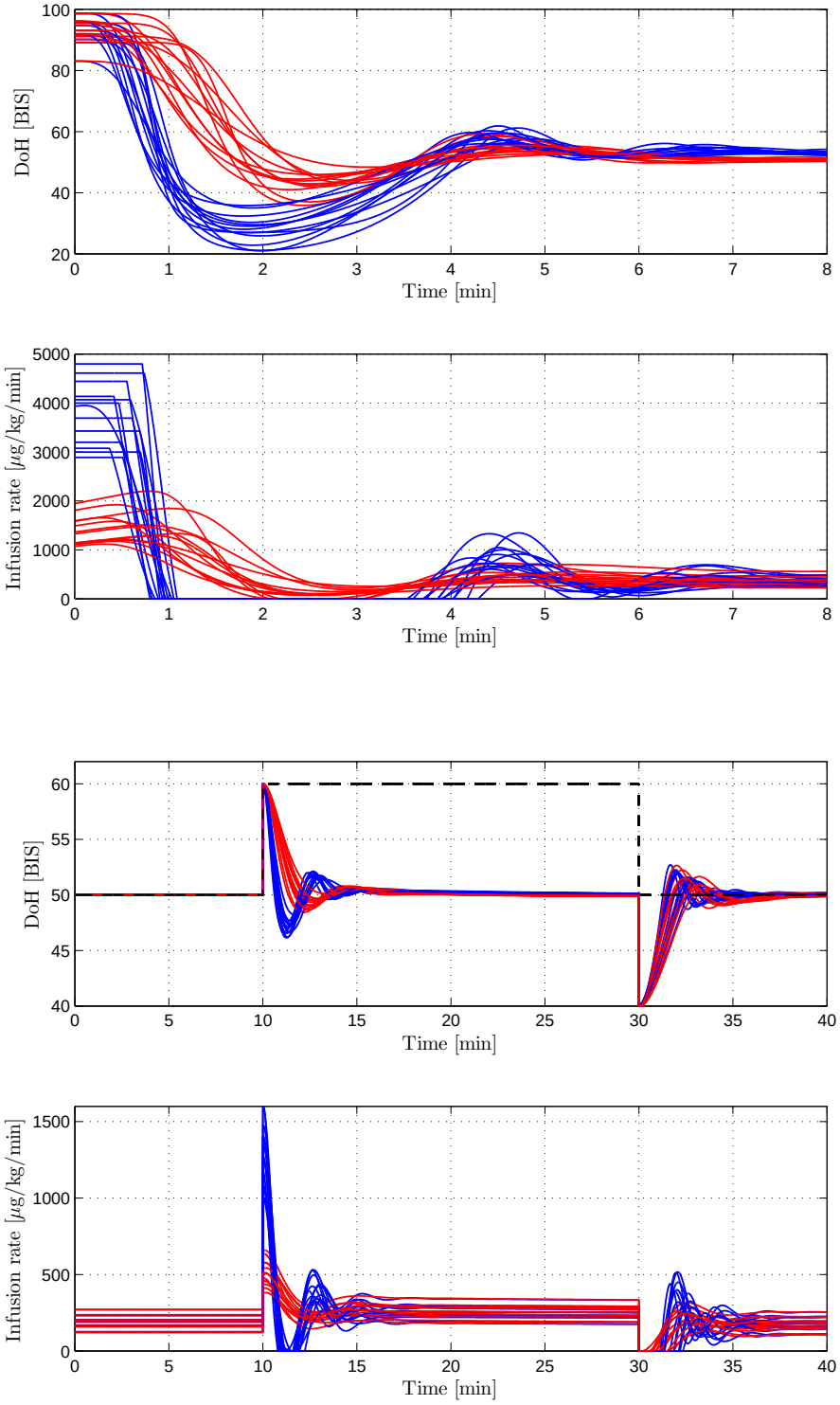

Figure 9: Simulated patients response to propofol infusion for set-point following (top) and disturbance rejection (bottom) tasks. Maximum pump rate of 240.00 [mg/min]. Optimal set-point tuning (red), and optimal disturbance tuning (blue).

troller outperforms also the two-degree-of-freedom PID controller and the fractional-order controller in [17] (although the latter has been tested on a different set of patients). The same conclusion can be derived by analyzing the results shown in [16] where a model predictive controller and an internal model control approach have been compared. The performance obtained with our PID controller is better when compared to the results presented in [19, 29, 32].
By contrast, the results obtained for the maintenance phase cannot be compared straightforwardly with those presented in the previously mentioned papers because a different disturbance signal has been employed. Note again that here we have used a simple step signal as a disturbance in order to facilitate the evaluation of the disturbance rejection performance of the controller. Nevertheless, when analyzing the results, one may conclude that the performance obtained with a PID controller specifically tuned for this task is fully consistent with that obtained by using other approaches. This confirms the necessity of using a gain scheduling strategy in the control algorithm. In particular, the use of disturbance rejection tuning for set-point tracking task generates a considerable loss of performance. Indeed, because of the aggressive controller tuning, it is likely to obtain a large overshoot.

6 Conclusions

The use of PID controllers for the dosing of propofol to control the depth of hypnosis in general anesthesia has been thoroughly analyzed in this paper. In particular, the tuning of the PID parameters has been performed by using genetic algorithms in order to minimize the worst-case integrated absolute error in a set of patient that is representative of a wide population. It has been stressed that it is necessary to employ a gain scheduling approach where different PID parameters are used in the induction and the maintenance phases. The importance of the derivative action has also been highlighted. Furthermore, the role of the low-pass filter to cope with the noisy BIS signal has been addressed by showing the trade-off between the effective filtering and the loss of performance in the set-point tracking.
The obtained results indicate that any other advanced control strategy employed in regulating anesthesia should be compared with optimally tuned PID controllers because they are capable to provide a fast induction time with an acceptable overshoot and a satisfactory disturbance rejection performance.

References

[1] J. M. Bailey, W. M. Haddad, Drug dosing control in clinical pharmacology, IEEE Control Systems Magazine, 25 (2)(2005) 35-51.

[2] Z. T. Zhusubaliyev, A. Medvedev, M. M. Silva, Bifurcation analysis for PID-controller tuning based on a minimal neuromuscular blockade model in closed-loop anesthesia, in: Proceedings IEEE International Conference on Decision Control, 2013, pp. 115-120.

[3] Z. T. Zhusubaliyev, A. Medvedev, M. M. Silva, Nonlinear dynamics in closed-loop anesthesia: Pharmacokinetic/pharmacodynamic model under PID-feedback, in: Proceedings American Control Conference, 2014, pp. 5496-5501.

[4] Z. T. Zhusubaliyev, M. M. Silva, A. Medvedev, Automatic recovery from nonlinear oscillations in PID-controlled anesthetic drug delivery, in: Proceedings European Control Conference, 2015, pp. 2725-2730.

[5] G. A. Dumont, Monitoring the EEG for assessing depth of anesthesia, in: J. M. Ehrenfeld, M. Cannesson (Eds.), Monitoring Technologies in Acute Care Environments, Springer, London, 2014, pp. 127-147.

[6] G. N. C. Kenny, H. Mantzaridis, Closed-loop control of propofol anaesthesia, British Journal of Anaesthesia, 83 (2005) 223-228.

[7] S. Bibian, Automation in clinical anesthesia, Ph.D. dissertation, University of British Columbia, Calgary, 2006.

[8] T. Zikov, S. Bibian, G. A. Dumont, M. Huzmezan, C. R. Ries, Quantifying cortical activity during general anesthesia using wavelet analysis, IEEE Transactions on Biomedical Engineering, 53 (2005) 617-632.

[9] N. Liu, M. Le Guen, F. Benabbes-Lambert, T. Chazot, B. Trillat, D. I. Sessler, M. Fischler, Feasibility of closed-loop titration of propofol and remifentanil guided by the spectral m-entropy monitor, Anesthesiology, 116 (2012) 286-295.

[10] C. H. Ting, R. H. Arnott, D. A. Linkens, A. Angel, Migrating from target-controlled infusion to closed-loop control in general anesthesia, Computer Methods and Programs in Biomedicine, 75 (2004) 127-139.

[11] M. L. Lindholm, S. Traff, F. Granath, S. D. Greenwald, A. Ekbom, C. Lennmarken, R. H. Sandin, Mortality within 2 years after surgery in relation to low intraoperative bispectral index values and preexisting malignant disease, Anesthesia and Analgesia, 108 (2) (2009) 508-512.

[12] C. F. Minto, T. W. Schnider, Contributions of PK/PD modeling to intravenous anesthesia, Clinical Pharmacology & Therapeutics, 84 (2008) 27-38.

[13] M. M. Silva, J. M. Lemos, A. Coito, B. A. Costa, T. Wigren, T. Mendonca, Local identifiability and sensitivity analysis of neuromuscolar

blockade and depth of hypnosis model, Computer Methods and Programs in Biomedicine, 113 (2014) 23-36.

[14] A. Abdulla, P. Wen, W. Xiang, The design and investigation of model based internal model control for the regulation of hypnosis, in: Proceedings IEEE International Conference on Nano/Molecular Medicine and Engineering, 2010, pp. 192-197.

[15] C. M. Ionescu, R. D. Keyser, B. C. Torrico, T. D. Smet, M. M. R. F. Struys, J. E. Normey-Rico, Robust predicitve control strategy applied for propofol dosing using BIS as a controlled variable during anesthesia, IEEE Transactions on Biomedical Engineering, 55 (9) (2008) 2161-2170.

[16] S. Yelneedi, L. Samavedham, G. P. Rangaiah, Advanced control strategies for the regulation of hypnosis with propofol, Industrial and Engineering Chemistry Research, 48 (2009) 3880-3897.

[17] G. A. Dumont, A. Martinez, J. M. Ansermino, Robust control of depth of anesthesia, International Journal of Adaptive Control and Signal Processing, 23 (2009) 435-454.

[18] A. Martinez, Robust control: PID vs. fractional control design, a case study, Master thesis, Instituto Tecnologico de Estudios Superiores de Monterrey, Mexico, 2000.

[19] J.-O. Hahna, G. A. Dumont, J. M. Ansermino, Robust closed-loop control of hypnosis with propofol using WAV_{CNS} index as the controlled variable, Biomedical Signal Processing and Control, 7 (2012) 517-524.

[20] H. Araujo, B. Xiao, C. Liu, Y. Zhao, H. K. Lam, Design of type-1 and interval type-2 fuzzy PID control for anesthesia using genetic algorithms, Journal of Intelligent Learning Systems and Applications, 4 (2014) 70-93.

[21] M. Janda, O. Simanski, J. Bajorat, B. Pohl, G. F. E. Noeldge-Schomburg, R. Hofmockel, Clinical evaluation of a simultaneous closed-loop anaesthesia control system for depth of anaesthesia and neuromuscular blockade, Anesthesia, 66 (2011) 1112-1120.

[22] W. M. Haddad, J. M. Bailey, T. Hayakawa, N. Hovakimyan, Neural network adaptive output feedback control for intensive care unit sedation and intraoperative anesthesia, IEEE Transactions on Neural Networks, 18 (2007) 1049-1066.

[23] F. N. Nogueira, T. Mendona, P. Rocha, Controlling the depth of anesthesia by a novel positive control strategy, Computer Methods and Programs on Biomedicine, 114 (3) (2014) e87-e97.

[24] N. Liu, E. M. Hafiani, M. Le Guen, Closed-loop anesthesia based on neuromonitoring, in: J. M. Ehrenfeld, M. Cannesson (Eds.), Monitoring Technologies in Acute Care Environments, Springer, London, 2014, pp. 275-279.

[25] A. R. Absalom, G. N. Kenny, Closed-loop control of propofol anaesthesia using bispectral index: performance assessment in patients receiving computer controlled propofol and manually controlled remifentanil infusions for minor surgery, British Journal of Anaesthesia, 90 (2003) 737-741.

[26] A. R. Absalom, N. Sutcliffe, G. N. Kenny, Closed-loop control of anesthesia using bispectral index, Anesthesiology, 96 (2002) 67-73.

[27] N. Liu, T. Chazot, A. Genty, A. Landais, A. Restoux, K. McGee, P. A. Laloe, B. Trillat, L. Barvais, M. Fischler, Titration of propofol for anesthetic induction and maintenance guided by the bispectral index: closed-loop versus manual control, Anesthesiology, 104 (2006) 686-695.

[28] G. D. Puri, B. Kumar, J. Aveek, Closed-loop anaesthesia delievery system (CLADS) using bispectral index; a performance assessment study, Anaesthesia and Intensive Care, 35 (2007) 357-362.

[29] K. van Heusden, G. A. Dumont, K. Soltesz, C. L. Petersen, A. Umedaly, N. West, and J. M. Ansermino, Design and clinical evaluation of robust PID control of propofol anesthesia in children, IEEE Transactions on Control Systems Technology, 22 (2)92014) 491-501.

[30] N. Liu, T. Chazot, S. Hamada, A. Landais, N. Boichut, C. Dussaussoy, B. Trillat, L. Beydon, E. Samain, D. I. Sessler, M. Fischler, Closed-loop coadministration of propofol and remifentanil guided by bispectral index: a randomized multicenter study, Anesthesia & Analgesia, 112 (2011) 546-557.

[31] A. Morley, J. Derrick, P. Mainland, B. B. Lee, T. G. Short, Closed loop control of anaesthesia: an assessment of the bispectral index as the target of control, Anesthesia, 55 (2000) 953-959.

[32] K. Soltesz, J.-O. Hahna, T. Hagglund, G. A. Dumont, J. M. Ansermino, Individualized closed-loop control of propofol anesthesia: a preliminary study, Biomedical Signal Processing and Control, 8 (2013) 500-508.

[33] M. M. Struys, T. D. Smet, L. F. Versichelen, S. V. D. Velde, R. V. den Broecke, E. P. Mortier, Comparison of closed-loop controlled administration of propofol using bispectral index as the controlled variable versus standard practice controlled administration, Anesthesiology, 95 (2001) 6-17.

[34] L. Hemachandra, Target-controlled infusions, in: J. M. Ehrenfeld, M. Cannesson (Eds.), Monitoring Technologies in Acute Care Environments, Springer, 2014, pp. 281-287.

[35] H. Panagopoulos, K. J. Astrom, T. Hagglund, Design of PID controllers based on constrained optimisation, IEE Proceedings - Control Theory and Applications, 149 (2002) 32-40.

[36] M. T. Chan, B. C. Cheng, T. M. Lee, T. Gin, Bis-guided anesthesia decreases postoperative delirium and cognitive decline, Journal of Neurosurgical Anesthesiology, 25 (2013) 33-42.

[37] K. Leslie, T. G. Short, Low bispectral index values and death: the unresolved causality dilemma, Anesthesia and Analgesia, 113 (2011) 660-663.

[38] F. Padula, C. Ionescu, N. Latronico, M. Paltenghi, A. Visioli, G. Vivacqua, A gain-scheduled PID controller for propofol dosing in anesthesia, in: Proceedings 9th IFAC Symposium on Biological and Medical Systems, 2015, pp. 545-550.

[39] Z. T. Zhusubaliyev, A. Medvedev, M. M. Silva, Bifurcation analysis of PID-controlled neuromuscular blockade in closed-loop anesthesia, Journal of Process Control, 25 (2015) 152-163.

[40] M. Mitchell, An Introduction to Genetic Algorithms, MIT press, Cambridge, 1998.

[41] I. Nascu, A. Krieger, C. M. Ionescu, E. Pistikopoulos, Advanced model-based control studies for the induction and maintenance of intravenous anesthesia, IEEE Transactions on Biomedical Engineering, 62 (2015) 832-841.

[42] M. M. R. F. Struys, T. De Smet, S. Greenwald, A. R. Absalom, S. Binge, E. P. Mortier, Performance evaluation of two published closed-loop control systems using bispectral index monitoring: a simulation study, Anesthesiology, 95 (1) (2004) 6-17.

[43] T. W. Schnider, C. F. Minto, P. L. Gambus, C. Andresen, D. B. Goodale, S. L. Shafer, E. J. Youngs, The influence of method of administration and covariates on the pharmacokinetics of propofol in adult volunteers, Anesthesiology, 88 (1998) 1170-1182.

[44] T. H. Hallynck, H. H. Soep, J. A. Thomis, J. Boelaert, R. Daneels, L. Dettli, Should clearance be normalised to body surface or to lean body mass? British Journal of Clinical Pharmacology, 11 (5) (1981) 523-526.

[45] V. R. Segovia, T. Hagglund, K. J. Astrom, Measurement noise filtering for common PID tuning rules, Control Engineering Practice, 32 (2014) 43-63.

[46] K. Soltesz, On automation in anesthesia, Ph.D. dissertation, Lund University, Lund, 2013.

[47] K. J. Åström, T. Hägglund, Advanced PID Control, ISA Press, Research Triangle Park, 2006.